



PROJECT MUSE®

---

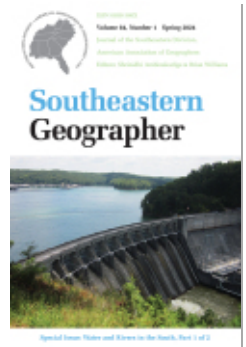
## UAV Imagery for Measuring Large Wood Volume and Distribution: Ground Truthing Results and Sources of Error

Joshua W. Hess, Robert T. Pavlowsky, Toby Dogwiler

Southeastern Geographer, Volume 64, Number 1, Spring 2024, pp. 11-29 (Article)

Published by The University of North Carolina Press

DOI: <https://doi.org/10.1353/sgo.00001>



➔ *For additional information about this article*

<https://muse.jhu.edu/article/920705>

# UAV Imagery for Measuring Large Wood Volume and Distribution: Ground Truthing Results and Sources of Error

**JOSHUA W. HESS**

*Ozarks Environmental and Water Resources Institute,  
Missouri State University, 901 S National Ave  
Springfield MO 65897*

**ROBERT T. PAVLOWSKY**

*Ozarks Environmental and Water Resources Institute,  
Missouri State University, 901 S National Ave  
Springfield MO 65897*

**TOBY DOGWILER**

*Missouri State University, 901 S National Ave Springfield MO 65897*

## HIGHLIGHTS:

- DSMs from UAVs and SfM photogrammetry can accurately depict stream valley topography ( $R^2 > 0.85$ ).
- Tree densities less than 400 trees/ha can be precisely measured using UAV orthoimagery.
- UAV-GIS methods can accurately measure individual pieces of LW with high precision.
- Canopy cover was the primary cause of LW detection and measurement errors using UAV imagery.

**ABSTRACT:** *UAV imagery offers great potential in determining precise environmental measurements. This study identifies and quantifies errors and their causes/sources between UAV imagery- and field-derived measurements of large wood (LW) and cross-sectional valley topography in several forested headwater stream valleys in the Ozark Highlands, Missouri. UAV imagery was collected at six sites following best practices for producing high resolution orthophotos and elevation models through Structure-from-Motion photogrammetry. Field-based measurements of LW were completed along 5 m wide valley cross-sections in which all LW > 1 m in length and 0.1 m in diameter were recorded. Topographic surveys were performed along the centerlines of the LW transects. The same assessments were performed using UAV imagery and ArcGIS. Our sites showed high ( $\geq 0.85$ )  $R^2$  values between field and UAV-GIS topographic surveys. Differences between measurements of LW dimensions tended to be larger with  $R^2$  ranging from 0.42 to 0.88. Overall 78 percent of standing trees and 60 percent of LW pieces were identified in the UAV imagery. The main source of detection and measurement error was due to vegetation/canopy cover. This study furthers our understanding of the applications and limitations of UAV derived data for environmental assessments.*

KEYWORDS: Riparian Forests, Missouri Ozarks, Digital Surface Model, Orthoimagery, GIS

## INTRODUCTION

Large wood (LW), defined here as any piece of wood (branch, root wad, tree trunk) greater than 1 meter in length and 0.1 meter in diameter, has well documented ecological and geomorphic functions in fluvial environments, providing hydraulic roughness, stream bed and bank erosion resistance, and landform stability (Hupp and Osterkamp, 1996; Hauer and Smith, 1998; Tal et al., 2004; Kupfer et al., 2008; Lininger et al., 2017; Martin et al., 2016; Stout et al., 2018; Martin et al., 2021). LW is typically quantified through direct measurement during field surveys, which can be time and resource intensive (Sanhueza et al., 2022). Recently, new methodologies for quantifying LW using Unoccupied Aerial Vehicles (UAVs), Structure-from-Motion (SfM) photogrammetry, and geographic information systems (GIS) have started to emerge (Gerke et al., 2019; Spreitzer et al., 2019; Sanhueza et al., 2019; Sanhueza et al., 2022). However, with only a limited number of studies using UAV-SfM technology to quantify LW, further evaluation of the data that UAV-SfM products can provide is necessary to have confidence in the application of the new methodologies.

Over the last couple of decades UAVs and SfM photogrammetry have been increasingly incorporated into environmental monitoring protocols as they provide the ability to rapidly assess environmental phenomena for relatively low cost while delivering high resolution imagery products (Quilter and Anderson, 2000; Dandois and Ellis, 2010; Anderson and Gaston, 2013; Hostens et al., 2022). These products, geo-rectified orthoimagery and digital surface models (DSMs), allow for accurate measurement of real-world three-dimensional features and therefore have been applied to a range of applications, including assessing biomass, habitat quality, biodiversity, and natural disasters/disturbances (Dandois and Ellis, 2010; Getzin et al., 2012; Fonstad et al., 2013; Watanabe and Kawahara, 2016; Hostens et al., 2022). Specifically, UAV-SfM products have shown great applicability for accurately depicting topography and quantifying a variety of forest characteristics (Getzin et al., 2012; Watanabe and Kawahara, 2016; Mohan et al., 2017; Guerra-Hernández et al., 2021; Finn et al., 2022). For example, in a comparison of cross-sections derived from field data and a UAV-SfM DSM, one study found an average elevation difference of 4 cm and a maximum difference of 7 cm (Watanabe and Kawahara, 2016). Limits to the imagery provided by the UAV came from vegetation which prevented accurate ground level data from being acquired and increased errors between the field cross-section and UAV-SfM DSM (Watanabe and Kawahara, 2016). UAV-SfM products have also been used to accurately measure and identify tree canopy heights and areas, individual trees, and other aspects of forest health through manual identification and automated processes (Getzin et al., 2012; Mohan et al., 2017; Guerra-Hernández et al., 2021; Finn et al., 2022).

Recently UAV-SfM methodologies have shown promising results for accurately extracting LW jam (three pieces of LW in contact) volumes. Through the use of ArcGIS

and Agisoft Metashape LW jam volumes derived from UAV-SfM DSMs have been estimated within 13 percent of measured field volumes (Sanhueza et al., 2022). However, the overestimation could be high (495 percent) depending on the method and software used to quantify the volume (Sanhueza et al., 2022). Another study used terrestrial photography and SfM photogrammetry to estimate LW jam volume but only examined two LW jams and did not analyze measurement errors of individual LW pieces (Spreitzer et al., 2019). In these examples, the volume of the LW jam was digitally or manually delineated and then semi-automatedly extracted from the DSM. This approach could result in the inclusion of background data (rocks, debris, organic matter) in the volumetric calculation increasing error (Spreitzer et al., 2019; Sanhueza et al., 2022). These studies have shown that the volume of LW jams can be estimated using UAV-SfM products. However, these studies do not assess the detection of LW in UAV imagery compared to field surveying or the dimensions of individual pieces of LW. Thus, there is a need for further evaluation of the data that UAV-SfM products can provide for LW and geomorphic surveying.

This study examines the intersection of forest and fluvial environments in riparian forests. It examines the application of UAVs for quantifying large wood and measuring cross-sectional stream valley topography. The need for rapid evaluation of LW distribution and geomorphic analysis through UAVs and SfM photogrammetry in this study comes after a >500-year flood event occurred in April 2017 in the Ozark Highland region of southern Missouri (Heimann et al., 2018). Three previous studies have examined various aspects of this flood event in the same study areas (Martin et al., 2021, Hostens et al., 2022, and Pavlowsky et al., 2023). Hostens et al. (2022) focused on identifying the best procedure for acquiring UAV imagery to ensure the highest accuracy of orthophotos and digital surface models in a steep, densely forested environment that poses image processing challenges. The other studies focused on quantifying LW loads in the active channel (Martin et al., 2021) and on floodplains, terraces, and secondary channel chutes (Pavlowsky et al., 2023) as well as reconstructing flood flows and examining post flood geomorphology (Martin et al., 2021 and Pavlowsky et al., 2023). Preliminary comparisons between GIS and field derived counts of LW at the sites were also quantified by Pavlowsky et al. (2023) to make a correction for LW loads and their relationship to geomorphic variables. However, analysis of detection and measurement errors of LW and cross-sectional valley topography between field and GIS methods was not conducted.

The objectives of this study are to (i) assess differences in cross-sectional stream topography between field surveying and UAV DSMs; (ii) quantify large wood detection differences between field and GIS (using UAV orthoimagery) observations; and (iii) assess differences in diameter, length, and volume measurements of large wood between field and GIS methods. UAVs have the potential to reduce time spent in the field conducting environmental assessments, thus saving time and resources (Sanhueza et al., 2022). However, further understanding is needed of the limitations of the data that UAVs can provide. This study contributes to our understanding of the capabilities and limitations

of UAVs in detecting and measuring LW and cross-sectional valley topography in a relatively rugged mid-continent forested environment.

## STUDY AREA

The North Fork of the White River watershed (1,453 km<sup>2</sup>) is in the Salem Plateau subdivision of the Ozark Plateau physiographic region of south-central Missouri (Figure 1). The watershed is composed of Ordovician aged horizontally bedded dolomite and sandstone geologic units. The Jefferson City and Cotter Dolomite form ridgetops, the Roubidoux Formation forms valleys, and the Gasconade Dolomite is present in valleys in lower portions of the watershed (Miller and Wilkerson, 2001). Upland soils form in thin loess deposits and dolomite residuum and contain large amounts of chert (Miller and Wilkerson, 2001). The acidic residuum is favorable for shortleaf pine (*Pinus echinata*) which in addition to several species of oak (*Quercus*) and hickory (*Carya*) compose most tree species in the watershed, which is 60 percent forested (Miller and Wilkerson, 2001; Stambaugh et al., 2002). The Ozark Highlands have a temperate climate with a mean annual temperature of 15 °C (Adamski, 1995). The region receives 120 cm of precipitation annually, with most events occurring in the spring (Adamski, 1995). Over the last thirty years, the frequency of intense precipitation events (> 7.5 cm/day) has increased significantly in the Ozark Highlands which has been increasing peak streamflow (Heimann et al., 2018).

In late April 2017, a storm system produced record-breaking precipitation across the Midwest United States. The storm generated 20 – 30 cm of rainfall over a 48-hour period from April 28 – 30, 2017 in the North Fork of the White River watershed (US Department of Commerce, 2017). The torrential rainfall led to widespread flooding in southern Missouri with twenty-one peak-of-record stream flows recorded at United States Geological Survey (USGS) stream gages (Heimann et al., 2018). On the North Fork of the White River the USGS stream gage near Tecumseh, Missouri (USGS 07057500) recorded a peak discharge over 5,000 m<sup>3</sup>/s, which the USGS estimated to have an annual exceedance probability of less than 0.2 percent (Heimann et al., 2018).

The extreme nature of the flood event provided a “once in a lifetime” opportunity to investigate the effects of the flood on stream channel geomorphology and riparian forest damage, including LW distribution. Six study reaches on tributaries of the North Fork of the White River were selected that were on public land within the Mark Twain National Forest with drainage areas ranging from 4.5 km<sup>2</sup> – 124.2 km<sup>2</sup> (Table 1). The sample reaches varied in size and ranged from 119 m in length to 766 m, approximately 15 – 20 channel widths in length (Rosgen, 1996) (Table 1). The valley floor areas assessed at each sample reach ranged in area from 0.3 to 4.8 hectares (Table 1). All the reaches were surrounded by forested land and their watersheds were also primarily forested except for Upper Tabor Creek which drains 52 percent agricultural land (Table 1).

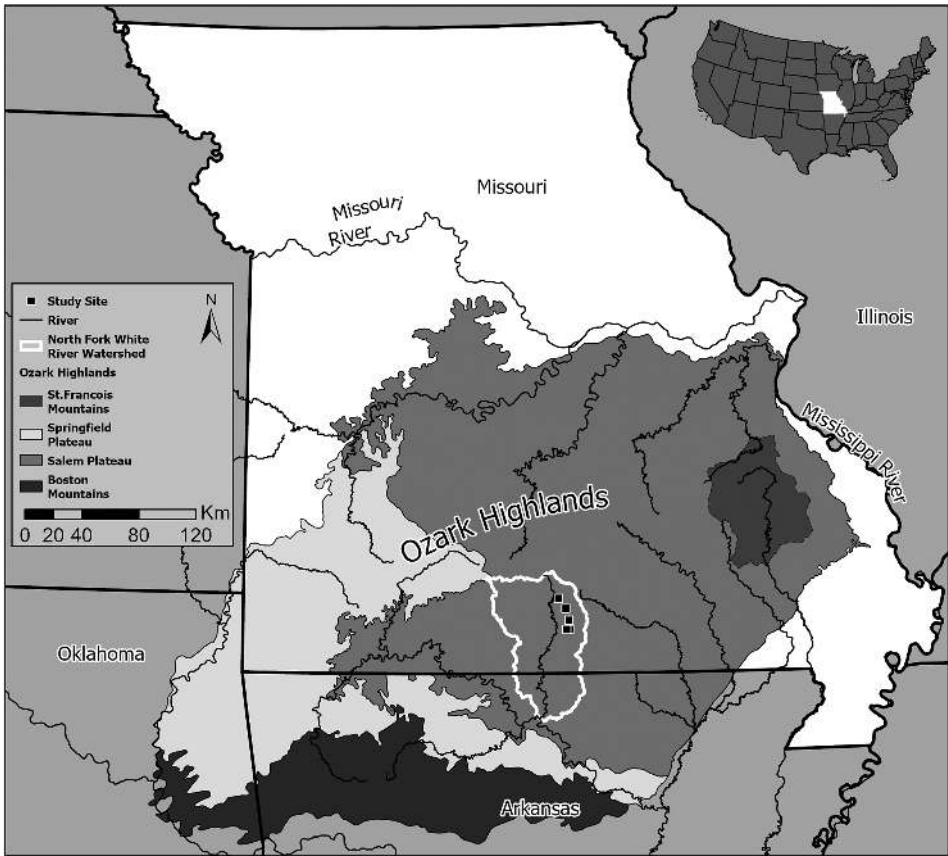


Figure 1. Regional setting of the study area.

Table 1. Study site characteristics.

	Dry Creek	Indian Creek	Lower Tabor Creek	Upper Tabor Creek	Spring Branch	Lick Branch
Drainage Area (km <sup>2</sup> )	124.2	101.6	65.4	54	49.1	4.5
Reach Length (m)	303	470	766	404	424	119
Reach Area (ha)	2.1	4.0	4.8	2.0	3.4	0.3
Watershed Land Use %						
Agriculture	31	16	45	52	19	13
Forest	64	79	50	42	78	86
Urban	4	3	4	5	2	1
Other	1	2	1	1	1	0

## METHODS

### *Field transects*

Cross-sectional topographic surveying of the stream channel and valley bottom morphology was performed in August 2018 using a pulled tapeline and auto-level to record landform dimensions and elevations (Rosgen, 1996). A Trimble Geo 7x GPS unit was used to record the endpoints of the transects. In April 2019, the same transects were used as a centerline for a 5 m wide sampling zone to compare standing trees and LW field distributions to UAV-GIS methods (Fujita et al., 2003; Allen et al., 2012). While one topographic survey was conducted at each site, an additional transect for surveying LW was added at Indian Creek and Spring Branch, and two were added at Lick Branch. Locations of all standing trees within the sample zone were recorded using a GPS unit (Kupfer et al., 2008; Stout et al., 2018). Large wood was recorded in the sample zone if the piece of wood was greater than 0.1 m in diameter and greater than 1 m in length (Kupfer et al., 2008; Lininger et al., 2017; Martin et al., 2016; Stout et al., 2018; Martin et al., 2021). Two diameter measurements were recorded, one at the midpoint of the LW piece (Cordova et al., 2007) and one at the midpoint of only the portion within the 5 m transect zone. This was performed to analyze variability in LW diameter. LW length was measured from the larger end (rootwad) until the piece tapered to less than 0.1 m in diameter (Stout et al., 2018). LW volume was calculated assuming a cylindrical shape.

### *UAV imagery field methods*

A DJI Phantom 4 Pro (UAV) was used to collect leaf-off aerial imagery during early March 2018, approximately ten months after the April flood event. Stream gage records during this time indicate one near bankfull flood occurred, which potentially could have transported relatively small pieces of LW in the channel but would not have affected LW on floodplains and higher elevation surfaces in the valley bottom. This imagery was used to create high resolution ( $< 8$  cm), geo-rectified orthophotos and digital surface models (DSMs) using Structure-from-Motion photogrammetry (Hostens et al., 2022). Two UAV flight plans, north-to-south and east-to-west, and camera angles,  $90^\circ$  (orthogonal) and  $70^\circ$  (oblique), were combined to produce the final orthoimages and DSMs of the sites (Hostens et al., 2022). The UAV was flown at approximately 108 m above ground level and images were collected with 80 percent front and side overlap (Hostens et al., 2022). Five to ten Ground Control Points (GCPs) were evenly distributed across the sample reaches (in locations visible to the UAV) to increase spatial accuracy, with the number of GCPs increasing with site area (Hostens et al., 2022). For large project areas, three GCPs per 100 images acquired by UAVs achieved high accuracy UAV-SfM products (Sanz-Ablanedo et al., 2018). The images were then processed in Agisoft Metashape, which identifies tie points in photographs taken from several perspectives to create three-dimensional shapes of objects that can be accurately measured (Fonstad et al., 2013; Hostens et al., 2022).

### *GIS methods*

The orthophotos and DSMs were input into ArcGIS and used to manually digitize LW along the sampled field transects (Figure 2). All LW extending into the 5 m wide valley

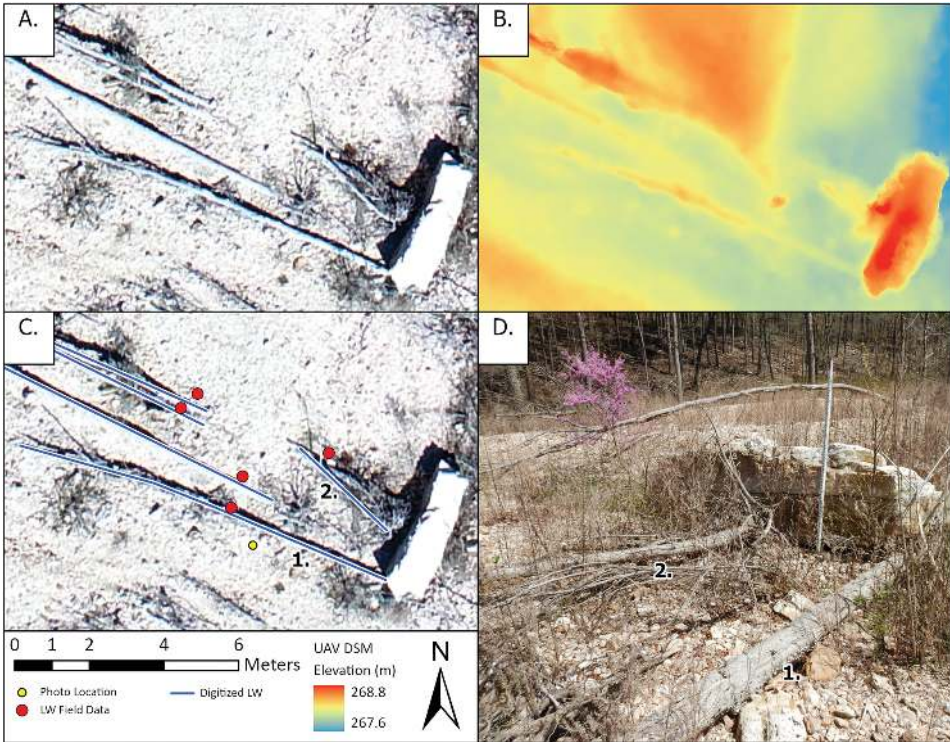


Figure 2. A portion of the Lower Tabor site transect sampling zone. A) UAV orthoimagery. B) UAV DSM. C) UAV orthoimagery with field and GIS LW identified – note numbered LW correspond with D) - LW piece #1 is 10 m long and 0.16 m in diameter. LW #2 is 3.5 m long and 0.20 m in diameter. D) Photograph of LW along the Lower Tabor transect.

transect zone was hand digitized as a line feature and attributed with a length and diameter measurement. Length of the digitized LW was measured using the “Calculate Geometry” function in ArcGIS. Diameter was measured using the “Distance” tool. Standing trees were digitized as point features in the approximate center of the tree canopy where branches could be seen radiating from. Standing tree density (#/ha) was calculated as the number of trees within the 5 m wide valley transect zone per the area of the zone in hectares. Manual digitization of aerial photographs through GIS platforms such as ArcGIS, are frequently used to identify features such as riverbanks and individual trees or plants (Winterbottom and Gilvear, 2000; Rhoades et al., 2009; Oddi et al., 2021). Although subjective, this relatively simple process offers an efficient way to quantify and analyze feature characteristics and spatial patterns (Oddi et al., 2021).

The recorded GPS points of the field locations of standing trees and LW pieces were matched with the nearest digitized feature in ArcGIS. In some cases where GPS points/LW were near one another, other attributes (length, diameter) were used to help identify

which piece of LW the GPS point belonged to. Once LW pieces were matched between the two methods using their location, individual measurements of LW diameter and length were compared. We refer to the difference between the GIS derived measurement (using UAV imagery) and the field measurement for the same piece of LW as measurement “errors”. Standing tree densities between the field survey and GIS analysis of UAV imagery were also compared.

## RESULTS

### *Valley bottom topography*

At all sites, the UAV DSM showed surface variability due to large wood, flood debris, vegetation, and standing tree canopies obstructing the ground surface from UAV photos. At Upper Tabor Creek, tree canopy areas from the UAV DSM were removed by hand and excluded data that was clearly showing standing trees 15-20 m in height above the ground surface. Vegetation on the ground along with flood and wood debris was not filtered from the cross-sections. However, there are several vegetation filtering algorithms that can be used to filter ground elevations from UAV derived point clouds (Anders et al., 2019). Vegetation, flood debris, and LW were avoided during the topographic field survey and therefore represent the ground surface.

At Indian Creek, the cross-section data required further correction before comparisons could be made. This was because after aligning the cross-sections with the thalweg points, the UAV derived data was oblique to the survey data (Figure 3). This was corrected using a simple equation, where the corrected UAV elevation was equal to the distance from the thalweg multiplied by the slope of the plane compared to the survey data (to correct for the obliqueness of the data) and added to the original UAV elevation.

Once corrected, cross-sectional surveys from the two methods showed good alignment, with  $R^2$  values between the elevation datasets greater than 0.85 at all the sites (Table 2).  $R^2$  values were highest at Lick Branch (0.98) and lowest at Indian Creek (0.85) (Table 2). Additionally, Root Mean Squares Errors (RMSE) were less than 0.39 m at all sites (Table 2). Lick Branch had the lowest RMSE, 0.15 m, due to the small amount of vegetation and debris on the valley floor. When the datasets by site were combined the  $R^2$  value was 0.999 and the RMSE was 0.32 m (Table 2). RMSE values up to 0.39 m are due to the vegetation, LW, and flood debris obstructing the ground surface. These errors were expected as we compared the UAV digital surface model (reflecting the surface including vegetation) to the field survey digital terrain model (reflecting the ground surface with no vegetation). However, the comparison of the UAV DSM to the field survey shows that UAV imagery processed through SfM photogrammetry can accurately depict cross-sectional stream valley morphology. These findings are similar to previous studies which have found that errors between field and UAV-DSMs are minimized when vegetation is short and sparse (Watanabe and Kawahara, 2016).

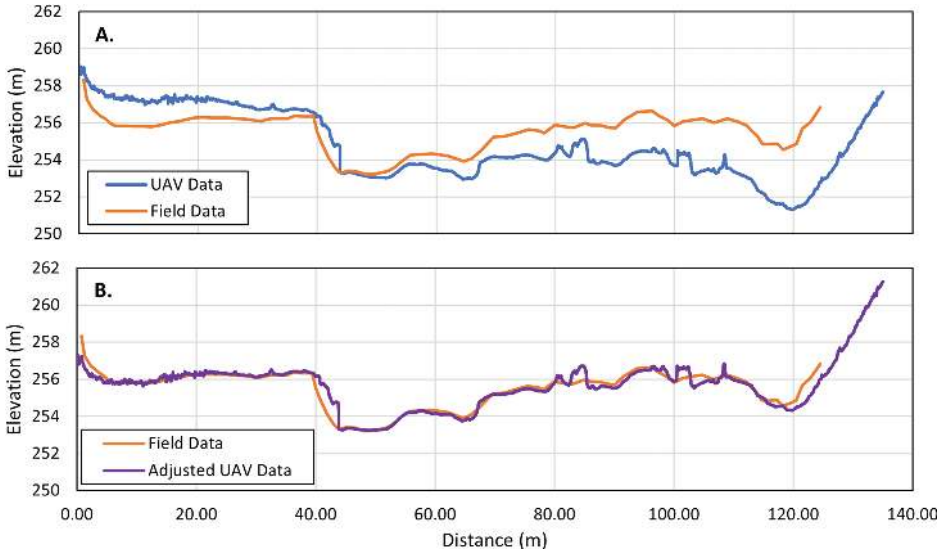


Figure 3. Comparison of field and UAV elevation data at Indian Creek. A) Unadjusted UAV Data. B) Adjusted UAV data.

Table 2. Coefficient of determination and root mean square errors between UAV-GIS and field cross-sections.

Site	R <sup>2</sup>	RMSE
Dry Creek	0.92	0.39
Indian Creek	0.85	0.39
Lower Tabor Creek	0.96	0.23
Upper Tabor Creek	0.97	0.29
Spring Branch	0.87	0.31
Lick Branch	0.98	0.15
All Sites	0.999	0.32

*Standing tree and LW detection*

Field surveys found seventy-three standing trees in the 5 m wide sample areas, while the GIS survey found fifty-seven in the UAV orthoimagery. Standing tree density (#/ha) in the sample areas found similar results with tree densities plotted on a 1:1 line for densities less than 400 trees/ha (Figure 4). Standing tree densities were greater than 400 trees/ha in field surveys on one transect at Lick Branch and one transect at Spring Branch (Table 3). Standing tree densities were underpredicted using the UAV

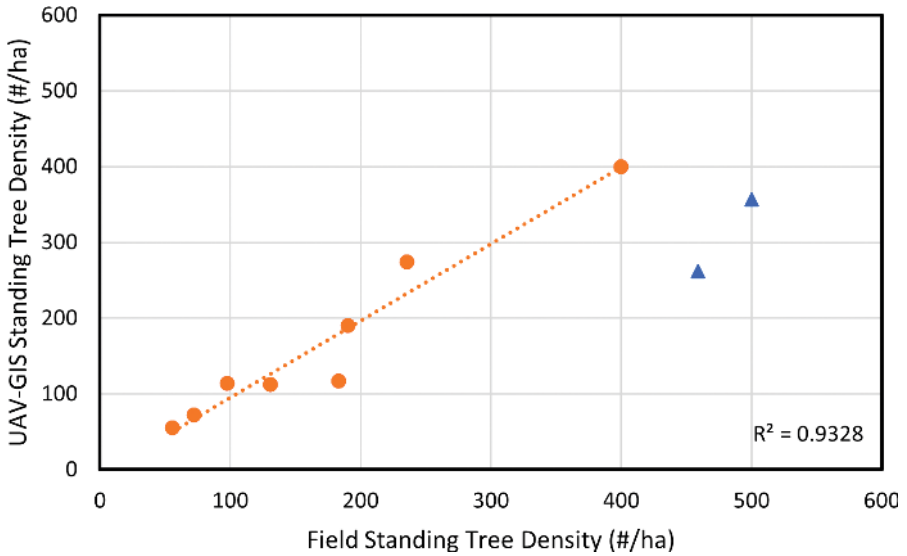


Figure 4. Field and UAV-GIS measurements of standing tree density. Triangle points represent sampled transects with standing tree density > 400 trees/ha that were excluded from the relationship.

Table 3. Detection of standing trees and large wood.

Site	Standing Tree			Large Wood				
	Field Survey Density (#/ha)	GIS Survey Density (#/ha)	Basal Area (m <sup>2</sup> /ha)	Field Survey (n)	GIS Survey (n)	Un-matched (%)	Field (m <sup>3</sup> /ha)	GIS (m <sup>3</sup> /ha)
Dry Creek	56	56	17.4	10	7	30	66	55
Indian Creek 1	131	112	17.6	13	7	46	53.3	39.3
Indian Creek 2	183	117	15.4	21	17	19	59.1	31.7
Lower Tabor Creek	72	72	9.9	28	18	36	61.4	43.6
Upper Tabor Creek	235	275	19.9	19	7	63	82.4	21.6
Spring Branch 1	98	114	4.4	20	13	35	79.9	56.2
Spring Branch 2	459	262	29.5	4	0	100	10.2	0
Lick Branch 1	400	400	68.5	6	4	33	NA	NA
Lick Branch 2	500	357	48.2	0	0	0	51.3	11.6
Lick Branch 3	190	190	2.5	0	0	0	NA	NA

orthoimagery and GIS when density was over 400 trees/ha due to being unable to visually distinguish individual trees from a mass of canopy branches in the orthoimagery.

Overall, 78 percent of standing trees found in field surveys were found in UAV orthoimagery. However, when only evaluating transects with standing tree densities less than 400 trees/ha, 93 percent of trees were identified. Forest basal areas of standing trees ranged from 3 to 69 m<sup>2</sup>/ha among the North Fork riparian transects (Table 3).

Table 4. Differences between field and UAV-GIS measurements of LW.

Site	Field vs UAV-GIS - All LW Length Errors (m)			Field vs UAV-GIS - LW Subset Length Errors (m)			Imagery Resolution (m)
	Avg	Max	Min	Avg	Max	Min	
Dry Creek	3.1	5.4	0.8	3.2	5.4	0.8	0.05
Indian Creek	3.1	16.3	0.3	1.1	3.2	0.3	0.05
Lower Tabor Creek	1.6	7.4	0.0	1.2	3.0	0.0	0.04
Upper Tabor Creek	1.8	4.3	0.0	1.8	1.8	1.8	0.03
Spring Branch	2.6	7.4	0.1	2.0	5.8	0.3	0.03
Lick Branch	5.5	9.5	0.9	NA	NA	NA	0.08

Site	Field vs UAV-GIS - Diameter Errors (m)			Field vs Field - Diameter Variability (m)			Imagery Resolution (m)
	Avg	Max	Min	Avg	Max	Min	
Dry Creek	0.01	0.04	0.00	0.05	0.27	0.00	0.05
Indian Creek	0.02	0.12	0.00	0.03	0.22	0.00	0.05
Lower Tabor Creek	0.02	0.10	0.00	0.04	0.26	0.00	0.04
Upper Tabor Creek	0.03	0.06	0.01	0.02	0.04	0.00	0.03
Spring Branch	0.03	0.05	0.00	0.04	0.08	0.00	0.03
Lick Branch	0.09	0.13	0.03	0.00	0.00	0.00	0.08

The results of this study overlap ranges reported for closed canopy oak and pine forests in the Ozark Highlands from 14-39 m<sup>2</sup>/ha (Hanberry et al., 2014) and 10-40 m<sup>2</sup>/ha (Hente, 2017). Field surveys found 121 pieces of LW within the sample transect zones (Table 3). Of those 121 pieces, 60 percent (73) were identified in UAV orthoimages. Along the transects, the percentage of undetected LW ranged from 19 percent at Indian Creek-2 to 100 percent at Spring Branch-2, where only four pieces of LW were found in the field survey (Table 3).

#### *LW diameter, length, and volume*

On average the two field measurements of LW diameter were within 0.03 m of each other and had a median difference of 0.01 m, with 90 percent of the measurements within 0.08 m. The maximum variability in field measurements of LW diameter was 0.27 m (Table 4). This comparison shows that diameter variability of LW pieces was generally low, with an average relative percent difference of 14 percent. The closest of the two diameter measurements to the UAV value was used to determine paired relationships for evaluation.

Comparisons between LW diameter values from field and UAV-GIS methods generally showed good agreement, with  $R^2 = 0.83$  and  $p\text{-value} < 0.01$  and plotted tightly along a 1:1 line (Figure 5A). Ninety percent of the paired field and UAV-GIS diameter measurements were within 0.06 m of each other. The average difference in diameter

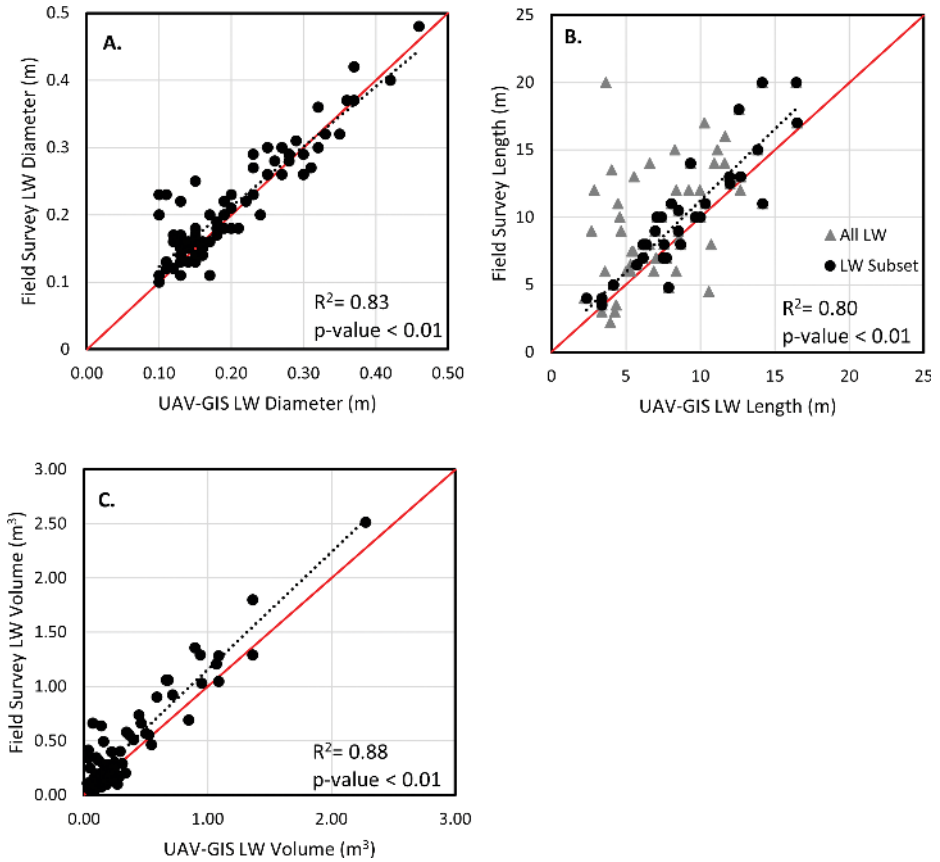


Figure 5. Field and UAV-GIS measurements of LW diameter (A), length (B), and volume (C). All LW data that was matched between field and UAV-GIS surveys were used in these figures. Additionally, Figure 5B uses a subset of the LW data that was unobstructed by canopy cover, vegetation, and flood debris to examine the UAV-GIS method to predict measured LW dimensions of “mostly visible” LW.

measurements was less than 0.03 m at all sites except for Lick Branch (Table 4). Lick Branch also had the largest minimum (0.03 m) and maximum (0.13) diameter errors (Table 4). Diameter measurement errors tended to increase as the spatial resolution of the UAV orthoimagery coarsened. Recall that all UAV orthoimagery had a spatial resolution of less than 0.08 m (Table 4). Differences in imagery resolution can be attributed to local variability of several factors at the sites including topography, surface texture (vegetation), lighting (time of day), wind speed and direction (Hostens et al., 2022). The average relative percent difference between diameter measurements was 14 percent. These results show that UAV orthoimagery can be used to accurately measure diameter on individual pieces of LW since differences between UAV-GIS and field measurements were typically similar to the variability of the log diameter.

Large wood length errors between paired field and UAV-GIS measurements were greater than diameter errors. When using the entire LW dataset ( $n = 73$ ),  $R^2$  values equaled 0.42 with the UAV-GIS method typically underpredicting LW lengths. Only 36 percent of the LW UAV-GIS length measurements were within 1 m of the field data. Average measurement error by site ranged from 1.6 m at Lower Tabor Creek to 5.5 m at Lick Branch (Table 4). The largest error was observed at Indian Creek with a difference in LW length of 16 m (Table 4). While diameter measurement errors between the two methods were mostly caused by sample location and imagery resolution, length errors were caused by canopy obstruction and burial by sediment, flood debris, or by other LW. Therefore, errors in length measurements are primarily due to the apparent shortening of the log due to visual obstruction.

Measurement errors of LW length between the two methods were further assessed using an unobstructed subset of the dataset ( $n = 34$ , 47 percent) in which the LW in the UAV orthoimagery was visually inspected and determined to be mostly unobstructed by canopy cover, vegetation, and flood debris. The  $R^2$  value increased to 0.80 ( $p$ -value  $< 0.01$ ) when using this subset of LW data and plotted near a 1:1 trendline but UAV-GIS methods slightly underpredicted field measurements (Figure 5B). Fifty percent of length measurements were within 1 m and 90 percent within 4.1 m. By site, average length errors were greatest at Dry Creek (3.2 m) and lowest at Indian Creek (1.1 m) (Table 4). Maximum length errors were greatest at Spring Branch which had one piece of LW underpredicted by 5.8 m (Table 4). The evaluation of the unobstructed subset of paired length data provided better insight into the use of UAV imagery to detect individual LW lengths. However, the average measurement error was still 1.7 m. Some of this error may be because of the angle of LW relative to the ground as oblique pieces of wood could appear shorter in aerial imagery, however, these effects were not quantified. The average relative percent difference for all measurements of LW length was 32 percent and 18 percent using only the “unobstructed” subset. In general, the relative percent difference increased as measurements of LW length in UAV imagery decreased.

Using UAV orthoimagery and GIS methods to calculate the volume of individual LW pieces produced an  $R^2$  of 0.88 ( $p$ -value  $< 0.01$ ) (Figure 5C). Average paired volume measurement errors were within  $0.14 \text{ m}^3$  with a maximum difference of  $0.59 \text{ m}^3$  and a minimum of  $0 \text{ m}^3$ . UAV-GIS calculations of LW volume typically underpredict the field volume of LW due to the underprediction of LW length (Figure 5B & 5C). When using the subset of LW data, showing mostly unobstructed LW, the  $R^2 = 0.96$ . The high  $R^2$  value indicates that the UAV-GIS measurements could accurately estimate LW loads, especially when only using data that is unobstructed from view in the UAV imagery. LW loads across the valley floor ranged from 10.2 to  $82.4 \text{ m}^3/\text{ha}$  which is similar to previous studies of LW in Missouri that have found LW loads ranging from 7 to  $234 \text{ m}^3/\text{ha}$  (Table 3) (Martin et al., 2016, Martin et al., 2021).

## DISCUSSION

An evaluation of the specific types of errors involved in this study was performed to better understand the sources of differences between field and UAV LW detection and

measurements. Visual inspection of UAV imagery, field notes, and photographs was used to assess LW detection errors. Of the 48 pieces of LW that were not identified in the UAV orthoimages, 71 percent were obstructed by canopy cover, 13 percent were buried by sediment, 8 percent were thought to have been transported or newly deposited in the time between the UAV imagery collection and the field survey, 4 percent were unidentifiable due to image processing, and 4 percent were unable to be identified due to the accuracy of the GPS in the field. Therefore, the majority of LW detection errors (85 percent) are caused by other objects (canopy cover and sediment) concealing LW in the imagery. Only 4 percent of detection errors were associated with image processing. This is caused by a lack of unique features in photos resulting in blurred patches in the final orthoimagery. This only occurred at the Spring Branch-2 site where the standing tree density was greater than 400 trees/ha (Table 3). As expected, this analysis indicates that most errors are related to visual obstruction of the LW piece by material on the ground or a dense overhead canopy. Moreover, few errors (< 10 percent) were due to image processing or errors in GPS readings.

The overall detection accuracy of 60 percent of LW and 78 percent of standing trees reported in the present study can be increased in future applications by using improved methods and sampling procedures. However, this error rate is expected given the relatively dense canopy present in sample reaches (Belmonte et al., 2019). Under optimal conditions to identify standing shrubs or trees, 99 percent accuracy was produced using high resolution UAV imagery and manual digitizing to identify tree and shrub encroachment into grasslands with no forest canopy (Oddi et al., 2021). Other studies using similar methods to this study have achieved 85-90 percent detection rates for individual (standing) trees in low to moderate canopy cover (Mohan et al., 2017; Finn et al., 2022). While detection rates of LW have been found to be 68 percent in moderate canopy cover and nearly 90 percent with low to open canopy cover (Gerke et al., 2019; Sanhueza et al., 2019).

Measurement errors between UAV and field methods may also be affected by sampling time due to fluvial transport of LW and human interference. While leaf-off UAV imagery was collected in March 2018, field verification of LW in the sample transects occurred in April 2019, thirteen months after UAV images were collected. During this time, according to the USGS stream gage downstream of the sites, one bank-full flood event occurred. This event could have deposited new LW from upstream into our sample zones and transported LW that was within the zone downstream. This is supported by a 17.5 m long piece of LW present in the UAV orthoimagery in the active channel at Indian Creek that was not present during the LW field sampling. At Spring Branch, additional inputs of LW were also identified. In one area outside of the sample transects a tree near the bank of the stream could be seen slightly leaning over in UAV orthoimagery. During field surveys the tree had fallen into the stream.

These results are also affected by human interference as evidence of cut logs and burning was present at some of the sites, resulting in several pieces of LW identified in the UAV imagery that were not found in field surveys. At Dry Creek, Indian Creek, and

Lower Tabor Creek cut logs were observed near the sample reach. At the Dry Creek site, the recreational Ozark Trail crosses the reach and logs may have been cut to clear the trail. Logs at other sites may have been cut for fuel. The reduction of wood loads in riparian areas by human activities is a well-documented occurrence, with wood removed for navigation and flood mitigation (Wohl et al., 2019). At Upper and Lower Tabor Creek, there was also evidence of prescribed burning, which the Forest Service typically performs in February or March as a forest management practice.

Further errors could also be associated with GPS accuracy and sampling procedures. GPS accuracy was typically near 1 m, but LW distribution could be very dense and only one point was recorded per LW piece. In some cases, LW was directly above and aligned with other pieces of LW. Thus, sampling times and practices likely affected measurement errors between the two methods. To reduce these errors in the future, field sampling and UAV image collection should occur at the same time. Additionally, to increase the confidence of matching pieces of LW with field and UAV-GIS techniques, a GPS unit could be used to delineate LW as line features or as two endpoints in the field, that way more precise information is collected that can be used to match the locations of LW pieces between the two methods.

## CONCLUSIONS

This study compared orthoimagery and digital surface models (DSMs) derived from Unoccupied Aerial Vehicles (UAVs) and Structure-from-Motion (SfM) photogrammetry to field surveys of cross-sectional stream valley topography and detection and measurement of large wood (LW). Few studies have used UAVs to detect and measure LW (Gerke et al., 2019; Spreitzer et al., 2019; Sanhueza et al., 2019; Sanhueza et al., 2022) and therefore further study of their limitations is necessary for understanding the data they can provide.

UAV orthoimagery and digital surface models were able to accurately depict cross-sectional stream valley topography in a densely forested and relatively steep valley environment. Additionally, these products were able to identify standing trees and large wood and derive accurate measurements of LW diameter, length, and volume. Differences in the valley bottom topography between the two methods came from vegetation, LW, and flood debris which are known to increase elevation errors. Detection errors of standing trees and LW are mostly due to canopy or other debris cover, thus detection rates decrease as canopy cover/tree density increases. Measurement errors of LW diameter relate to the natural variability of LW logs and sample location on the piece. Length measurement errors are generally caused by visual or camera view obstructions, causing an underpredicting of total length. Applications of UAVs for detecting LW loads are best when canopy cover is reduced, exposing all or most of LW in the orthoimagery. This work furthers our understanding of the use of UAVs for assessing LW and stream morphology. Our results support the use of UAVs to rapidly assess environments after natural disasters, through cost and time efficient methods.

## REFERENCES CITED

- Adamski, J.C., Petersen, J.C., Freiwald, D.A., and Davis, J.V. 1995. Environmental and hydrologic setting of the Ozark Plateaus study unit, Arkansas, Kansas, Missouri, and Oklahoma. USGS Water-Resources Investigations Report, 94–4022. <https://doi.org/10.3133/wri944022>
- Allen, M.S., Thapa, V., Arévalo, J.R., and Palmer, M.W. 2012. Windstorm damage and forest recovery: accelerated succession, stand structure, and spatial pattern over 25 years in two Minnesota forests. *Plant Ecology* 213, 1833–1842. <http://dx.doi.org/10.1007/s11258-012-0139-9>
- Anders, N., Valente, J., Masselink, R., and Keesstra, S. 2019. Comparing filtering techniques for removing vegetation from UAV-based photogrammetric point clouds. *Drones*, 3(3), 61. <https://doi.org/10.3390/drones3030061>
- Anderson, K., and Gaston, K.J. 2013. Lightweight unmanned aerial vehicles will revolutionize spatial ecology. *Frontiers in Ecology and the Environment*, 11(3), 138–146. <https://doi.org/10.1890/120150>
- Belmonte, A., Sankey, T., Biederman, J. A., Bradford, J., Goetz, S. J., Kolb, T., and Woolley, T. 2019. UAV-derived estimates of forest structure to inform Ponderosa Pine Forest Restoration. *Remote Sensing in Ecology and Conservation*, 6(2), 181–197. <https://doi.org/10.1002/rse2.137>
- Cordova, J.M., Rosi-Marshall, E.J., Yamamuro, A.M., and Lamberti, G.A. 2007. Quantify, controls and functions of large woody debris in Midwestern USA streams. *River Research and Applications* 23, 21–33. <https://doi.org/10.1002/rra.963>
- Dandois, J.P., and Ellis, E.C. 2010. Remote Sensing of Vegetation Structure Using Computer Vision. *Remote Sensing* 2, 1157–1176. <https://doi.org/10.3390/rs2041157>
- Finn, A., Kumar, P., Peters, S., and O’Hehir, J. 2022. Unsupervised spectral-spatial processing of drone imagery for identification of Pine Seedlings. *ISPRS Journal of Photogrammetry and Remote Sensing*, 183, 363–388. <https://doi.org/10.1016/j.isprsjprs.2021.11.013>
- Fonstad, M.A., Dietrich, J.T., Courville, B.C., Jensen, J.L., and Carbonneau, P.E. 2013. Topographic structure from motion: a new development in photogrammetric measurement. *Earth Surface Processes and Landforms* 38, 421–430. <https://doi.org/10.1002/esp.3366>
- Fujita, T., Itaya, A., Miura, M., Manabe, T., and Yamamoto, S. 2003. Canopy Structure in a Temperate Old-Growth Evergreen Forest Analyzed by Using Aerial Photographs. *Plant Ecology* 168, 23–29. <https://doi.org/10.1023/A:1024477227614>
- Getzin, S., Wiegand, K., and Schöning, I. 2012. Assessing biodiversity in forests using very high-resolution images and unmanned aerial vehicles. *Methods in Ecology and Evolution* 3, 397–404. <https://doi.org/10.1111/j.2041-210X.2011.00158.x>
- Guerra-Hernández, J., Díaz-Varela, R.A., Álvarez-González, J.G., and Rodríguez-González, P.M. 2021. Assessing a novel modelling approach with high resolution UAV imagery for monitoring health status in priority riparian forests. *Forest Ecosystems*, 8, 61. <https://doi.org/10.1186/s40663-021-00342-8>
- Hanberry, B.B., Jones-Farrand, D.T., and Kabrick, J.M. 2014. Historical open forest ecosystems in the Missouri Ozarks: reconstruction and restoration targets. *Ecological Restoration* 32 4, 407–416. <https://doi.org/10.3368/er.32.4.407>

- Hauer, F.R., and Smith, R.D. 1998. The hydrogeomorphic approach to functional assessment of riparian wetlands: evaluating impacts and mitigation on river floodplains of the U.S.A. *Freshwater Biology* 40, 517–530. <https://doi.org/10.1046/j.1365-2427.1998.00382.x>
- Heimann, D.C., Holmes, R.R., and Harris, T.E. 2018. Flooding in the southern Midwestern United States, April–May 2017. Open-File Report. <https://doi.org/10.3133/ofr20181004>
- Hente, M.L. 2017. Influence of prescribed burning on upland soil properties in Mark Twain National Forest, southeast Missouri Ozarks. Missouri State University Master's thesis in Geospatial Science, 3066.
- Hostens, D.S., Dogwiler, T., Hess, J.W., Pavlowsky, R.T., Bendix, J., and Martin, D.T. 2022. Assessing the Role of sUAS Mission Design in the Accuracy of Digital Surface Models Derived from Structure-from-Motion Photogrammetry, in K. Konsoer, M. Leitner, and Q. Lewis (eds.), *sUAS Applications in Geography*, Springer Nature, Geotechnologies and the Environment series volume 24. <https://link.springer.com/book/10.1007/978-3-031-01976-0>
- Hupp, C.R., and Osterkamp, W.R., 1996. Riparian vegetation and fluvial geomorphic processes. *Geomorphology* 14, 277–295. [https://doi.org/10.1016/0169-555X\(95\)00042-4](https://doi.org/10.1016/0169-555X(95)00042-4)
- Kupfer, J.A., Myers, A.T., Mclane, S.E., and Melton, G.N. 2008. Patterns of Forest Damage in a Southern Mississippi Landscape Caused by Hurricane Katrina. *Ecosystems* 11, 45–60. <http://dx.doi.org/10.1007/s10021-007-9106-z>
- Lininger, K.B., Wohl, E., Sutfin, N.A., and Rose, J.R. 2017. Floodplain downed wood volumes: a comparison across three biomes. *Earth Surface Processes and Landforms* 42, 1248–1261. <https://doi.org/10.1002/esp.4072>
- Martin, D.J., Pavlowsky, R.T., and Harden, C.P. 2016. Reach-scale characterization of large woody debris in a low gradient, Midwestern USA river system. *Geomorphology*, 262, 91–100. <https://doi.org/10.1016/j.geomorph.2016.03.005>
- Martin, D.J., Pavlowsky, R.T., Bendix, J., Dogwiler, T., and Hess, J. 2021. Impacts of an extreme flood on large wood recruitment and transport processes. *Physical Geography* [doi.org/10.1080/02723646.2021.1980958](https://doi.org/10.1080/02723646.2021.1980958)
- Miller, S.M., and Wilkerson, T.F. 2001. North Fork River Watershed Inventory and Assessment, Missouri Department of Conservation.
- Mohan, M., Silva, C., Klauberg, C., Jat, P., Catts, G., Cardil, A., Hudak, A., and Dia, M. 2017. Individual tree detection from unmanned aerial vehicle (UAV) derived canopy height model in an open canopy mixed conifer forest. *Forests*, 8(9), 340. <https://doi.org/10.3390/f8090340>
- Oddi, L., Cremonese, E., Ascari, L., Filippa, G., Galvagno, M., Serafino, D., and Cella, U.M. (2021). Using UAV imagery to detect and map woody species encroachment in a subalpine grassland: Advantages and limits. *Remote Sensing*, 13(7), 1239. <https://doi.org/10.3390/rs13071239>
- Pavlowsky, R.T., Hess, J.W., Martin, D.J., Dogwiler, T., and Bendix, J. 2023. Large wood loads in channels and on floodplains after a 500-year flood using UAV imagery in Mark Twain National Forest, Ozark Highlands, Missouri. *Geomorphology*, 431, 108672. <https://doi.org/10.1016/j.geomorph.2023.108672>
- Quilter, M., and Anderson, V. 2000. Low Altitude/Large Scale Aerial Photographs: a Tool for Range and Resource Managers. *Rangelands* 22, 13–17. [http://dx.doi.org/10.2458/azu\\_rangelands\\_v22i2\\_quilter](http://dx.doi.org/10.2458/azu_rangelands_v22i2_quilter)

- Rhoades, E.L., O'Neal, M.A., and Pizzuto, J.E. 2009. Quantifying Bank erosion on the South River from 1937 to 2005, and its importance in assessing HG contamination. *Applied Geography* 29, 125–134. <https://doi.org/10.1016/j.apgeog.2008.08.005>
- Rosgen, D., 1996. *Applied river morphology*. Wildland Hydrology, Pagosa Springs, Colorado.
- Sanhueza, D., Picco, L., Ruiz-Villanueva, V., Iroumé, A., Ulloa, H., and Barrientos, G. 2019. Quantification of fluvial wood using UAVs and structure from motion. *Geomorphology* 345, 106837. <https://doi.org/10.1016/j.geomorph.2019.106837>
- Sanhueza, D., Picco, L., Paredes, A., and Iroumé, A. 2022. A faster approach to quantify large wood using uavs. *Drones*, 6(8), 218. <https://doi.org/10.3390/drones6080218>
- Sanz-Ablanedo, E., Chandler, J.H., Rodríguez-Pérez, J.R., and Ordóñez, C. 2018. Accuracy of Unmanned Aerial Vehicle (UAV) and SFM photogrammetry survey as a function of the number and location of ground control points used. *Remote Sensing* 10. <https://doi.org/10.3390/rs10101606>
- Spreitzer, G., Tunncliffe, J., and Friedrich, H. 2019. Using structure from motion photogrammetry to assess large wood (LW) accumulations in the field. *Geomorphology*, 346, 106851. <https://doi.org/10.1016/j.geomorph.2019.106851>
- Stambaugh, M.C., Muzika, R.M., and Guyette, R.P. 2002. Disturbance characteristics and overstory composition of an old-growth shortleaf pine (*Pinus echinata* Mill.) forest in the Ozark Highlands, Missouri, USA. *Natural Areas* 22, 108–119.
- Stout, J.C., Rutherford, I.D., Grove, J., Webb, A.J., Kitchingman, A., Tonkin, Z., and Lyon, J. 2018. Passive recovery of wood loads in rivers. *Water Resources Research* 54, 8828–8846. <https://doi.org/10.1029/2017WR021071>
- Tal, M., Gran, K., Murray, A.B., Paola, C., and Hicks, D.M. 2004. Riparian vegetation as a primary control on channel characteristics in multi-thread rivers. *Riparian Vegetation and Fluvial Geomorphology Water Science and Application* 43–58. <https://doi.org/10.1029/008WSA04>
- US Department of Commerce, NOAA, National Weather Service, 2017. Historic Flooding Event – 28–30 April 2017. National Weather Service
- Watanabe, Y., and Kawahara, Y. 2016. UAV Photogrammetry for Monitoring Changes in River Topography and Vegetation. *Procedia Engineering* 154, 317–325. <https://doi.org/10.1016/j.proeng.2016.07.482>
- Winterbottom, S.J., and Gilvear, D.J. 2000. A GIS-based approach to mapping probabilities of river bank erosion: Regulated River Tummel, Scotland. *Regulated Rivers: Research & Management* 16, 127–140. [https://doi.org/10.1002/\(sici\)1099-1646\(200003/04\)16:2<127::aid-rrr573>3.0.co;2-q](https://doi.org/10.1002/(sici)1099-1646(200003/04)16:2<127::aid-rrr573>3.0.co;2-q)
- Wohl, E., Kramer, N., Ruiz-Villanueva, V., Scott, D.N., Comti, F., Gurnell, A.M., Piegay, H., Lininger, K.B., Jaeger, K.L., Walters, D.M., and Fausch, K.D. 2019. The natural wood regime in rivers. *Bioscience* 69 (4), 259–273. <https://doi.org/10.1093/biosci/biz013>

---

JOSHUA HESS (joshhess@missouristate.edu) is a Research Specialist at Ozarks Environmental and Water Resources Institute at Missouri State University in Springfield, Missouri. His research focuses on applying GIS methodologies to assess watershed conditions and river systems.

DR. ROBERT PAVLOWSKY (BobPavlowsky@missouristate.edu) is a Distinguished Professor in the School of Earth, Environment, and Sustainability and the Director of Ozarks Environmental and Water Resources Institute at Missouri State University in Springfield, Missouri. His research interests include fluvial geomorphology and sedimentology, environmental geochemistry, and climate change and human impacts on watersheds and river systems.

DR. TOBY DOGWILER (TDogwiler@missouristate.edu) is the Department Head and a Professor in the School of Earth, Environment, and Sustainability at Missouri State University in Springfield, Missouri. His primary research focus is on the development and application of methodologies for drone-based remote sensing related to environmental, agricultural, and conservation problems.